

LASER HEATER DESIGN FOR THE CLARA FEL TEST FACILITY

A. D. Brynes*, S. P. Jamison, B. D. Muratori, N. R. Thompson, P. H. Williams
STFC Daresbury Laboratory & Cockcroft Institute, Warrington, UK

Abstract

We present considerations of microbunching studies in the CLARA (Compact Linear Accelerator for Research and Applications), the proposed UK FEL test facility under construction at Daresbury Laboratory. CLARA, a high-brightness electron linac, presents an opportunity to study the microbunching instability. A number of theoretical models have been proposed concerning the causes of this instability, and it has also been observed at various FEL facilities. We have applied these models to the CLARA FEL, and propose a suitable laser heater design which will provide flexibility in terms of the range of modes of operation for CLARA. We also propose a method for inducing and controlling the microbunching instability via pulse stacking of the photoinjector laser.

INTRODUCTION

CLARA is a 250 MeV FEL test facility under construction at Daresbury Laboratory [1]. A number of FEL schemes will be tested at CLARA, requiring short electron bunches to be generated using either velocity bunching or magnetic bunch compression. The microbunching instability, as observed at a number of FEL facilities which operate at short wavelength [2,3], could be studied on CLARA. The instability can be generated by a number of factors, such as shot noise, variations in the photoinjector laser pulse profile, or space charge modulations at low energy, causing small-scale variations along the longitudinal profile of the bunch, and is amplified due to collective effects such as longitudinal space-charge and coherent synchrotron radiation in dispersive regions. Any density modulation is amplified due to space-charge effects, and energy modulations are transformed into further density modulations in a magnetic bunch compressor. We present some analytical calculations of the microbunching gain in CLARA, and study the applicability of a laser heater to damp the instability.

GENERATION AND AMPLIFICATION OF MICROBUNCHES

Bunches of particles generated at a photocathode will have a slightly nonuniform current density (mostly due to shot-noise fluctuations), and certain collective effects can amplify these variations – the two most significant of which are longitudinal space-charge (LSC) and coherent synchrotron radiation (CSR). The amplification, or gain, in microbunching between two points in the machine is given by comparing the Fourier transform of the current profile of the bunch, or bunching factor, at these locations [4]:

$$G(k_0) = \frac{b(k_2, s_2)}{b(k_1, s_1)}, \quad (1)$$

* alexander.brynes@stfc.ac.uk

with $s_{1,2}$, $k_{1,2}$ the initial and final locations and modulation wavelengths, and b the bunching factor. Analysis of the gain spectrum provides information about the wavelengths at which the largest density fluctuations will be observed. Figure 1 shows the microbunching gain due to CSR in CLARA (using the method in [4]), for the short pulse FEL mode at 240 MeV. In this operating mode, the gain due to CSR is around an order of magnitude larger than that due to LSC. However, the effect of LSC may be more significant in the velocity bunching mode, where both the bunch energy and bunch length are relatively short for a longer period.

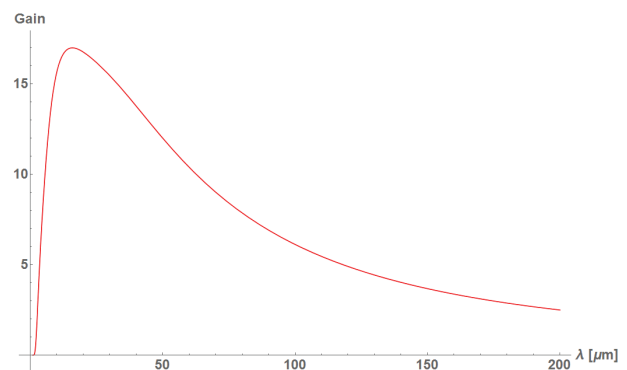


Figure 1: Gain due to CSR in CLARA bunch compressor.

INDUCING THE MICROBUNCHING INSTABILITY

Given that the expected microbunching gain is relatively small in comparison with higher-energy FEL facilities (see, e.g., [4, 5], where the gain can be up to 2 orders of magnitude larger), and that CLARA will provide a test-bed for future FEL technology in which microbunching may be an issue, we suggest that *inducing* the microbunching instability could provide an opportunity to perform detailed studies on which beam operation regimes are most likely to give rise to microbunching gain. There are several ways in which this could be done. The first is through shot noise amplification and the second is through a longitudinal density modulation [6] of the PI laser pulse. The first option seems difficult to achieve in a reproducible fashion and we therefore concentrate on the second. There are two known ways of achieving a longitudinally modulated laser pulse [6–8]. The first involves chirping the laser pulse by a grating pair and hence splitting this into two pulses, and the second involves the use of birefringent crystals.

A crystal such as α – BBO [8] has a large birefringence over a range of wavelengths from 190 to 3500 nm, and should be suitable for our purposes. There are many crystals

which can be used for this and, once we know the power involved, it will be possible to narrow the requirements further. The crystal is cut in such a way that its extraordinary axis (e), as opposed to the ordinary one (o) lies on its surface and is perpendicular to the incident laser pulse. With two types of initially coinciding polarised light, a retardation t (measured in ps) will develop after a propagation length l (measured in mm), in the crystal. This propagation length is given by: $l = ct/\Delta n$, with c the speed of light and Δn the difference in refractive index between the two axes of the crystal. By utilising a series of these crystals in the photoinjector laser line, a train of pulses can be produced at the photocathode. Provided that the laser power is not too high, we can use these or other birefringent crystals to imprint an initial modulation onto the PI laser pulse, which may then propagate downstream, although simulations are needed to confirm this.

CLARA LASER HEATER SYSTEM

The basic elements of the CLARA laser heater system comprise a laser, an undulator and a magnetic chicane, as illustrated in Fig. 2 and Table 1. The undulator period and gap are set to obtain a resonant interaction between the laser and the electron beam which ‘heats the beam’, imposing an energy modulation. The chicane provides a physical offset allowing the laser to be introduced along the electron trajectory. The second half of the chicane, or the exit dogleg, is also used to manipulate the electron bunch longitudinal phase space.

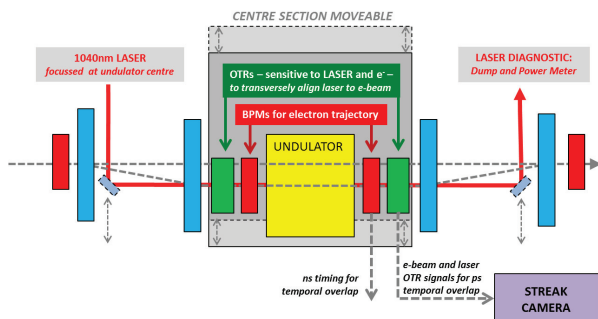


Figure 2: Schematic of laser heater system.

Gain Suppression with a Laser Heater

A laser heater has been utilised at various FEL facilities to increase the slice energy spread of the electron beam and remove microbunches [9, 10]. A resonant laser-electron interaction in an undulator within a dispersive region produces longitudinal modulation in the electron beam energy at the laser frequency, which creates an effective projected energy spread. Upon leaving the second half of the laser heater chicane, any structure in the beam is removed via dispersion, which converts this into an increase in the slice energy spread. The interaction between the laser and the electron beam in the laser heater undulator is strongest when the electron and laser radial rms sizes are similar.

Undulator and Laser

The laser wavelength is assumed to be 1040 nm and the beam energy at the laser heater will vary between 100 MeV and 200 MeV so the undulator must maintain resonance over this range. For 20 mm internal pipe diameter a conservative minimum undulator gap is 24 mm. With these constraints, assuming a planar, pure permanent magnet device with Nd-FeB blocks and a remanent field of $B_r = 1.2$ T the appropriate undulator period is found to be $\lambda_w = 60$ mm, giving an operating minimum undulator parameter of $a_w = 0.57$.

An approximation to the on-axis amplitude of the FEL modulation imposed by the laser is given by [11]:

$$\Delta\gamma_L(r) = \sqrt{\frac{P_L}{P_0} \frac{KL_u}{\gamma\sigma_r}} \left[J_0\left(\frac{K^2}{4+2K^2}\right) - J_1\left(\frac{K^2}{4+2K^2}\right) \right] \quad (2)$$

with P_L the laser power, $P_0 = (I_A mc^2)/e = 8.7$ GW, σ_r the rms laser spot size, and $J_{0,1}$ the Bessel functions of the first and second kind. Figure 3 shows the calculated energy modulation induced in a 100 MeV beam, using Eq. (2), for a range of laser powers and spot sizes, and undulator length $L = 0.48$ m, or 6 periods.

Figure 4 shows calculation of the microbunching gain suppression (without any induced microbunching) due to a laser heater-induced energy modulation of 30 keV, where the laser spot size is matched to the electron beam width. From Fig. 3, assuming for contingency a laser spot size as large as 500 μm , the required laser peak power is 10 MW. The laser pulse should also completely overlap the electron bunch longitudinally. The electron bunch length at the laser heater is $\sigma_z = 0.5$ mm giving $\sigma_r = 1.66$ ps and FWHM duration 3.9 ps. For easier longitudinal alignment it is proposed that the laser pulse length is twice as long as the electron bunch, giving the requirement $\Delta_{r,\text{laser}} = 8$ ps so the required pulse energy is $P \times \Delta_{r,\text{laser}} \approx 80 \mu\text{J}$.

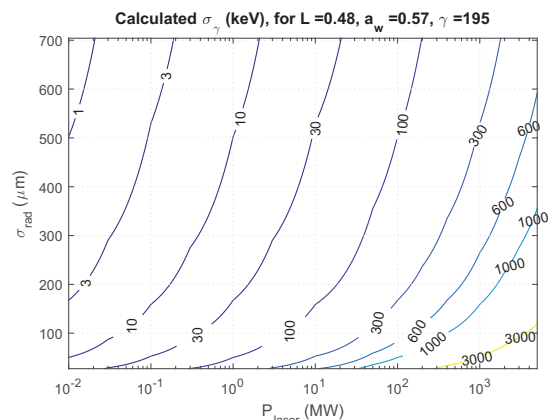


Figure 3: Left: calculated energy modulation induced in a 100 MeV beam, using Eq. (2), for a range of laser powers and spot sizes, and undulator length $L = 0.48$ m, or 6 periods.

Chicane, Beam Transport and Matching

The undulator was modelled in MAD8 [12] using a hard edge model to achieve the correct focusing in the horizontal

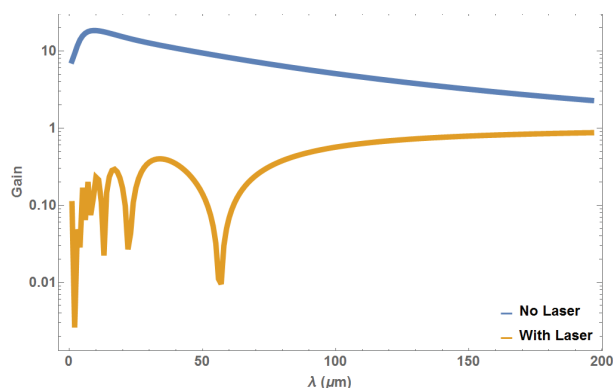


Figure 4: Comparison of microbunching gain with and without a laser heater.

Table 1: Laser Heater System Parameters

BEAM TRANSPORT	
Chicane magnet Length	10 cm
Chicane magnet bend angle	0 – 5 °
Beam energy	100 – 200 MeV
Emittance	0.5 mm–mrad
UNDULATOR	
Period	60 mm
Number of full periods	8
Total Length inc. end terminations	585 mm
Minimum undulator gap	24 mm
Undulator parameter	0.8 – 3.0
LASER	
Wavelength	1040 nm
Spot size σ_{rad} at undulator centre	$\leq 500 \mu\text{m}$
Pulse energy	80 μJ

plane. For the purposes of the modelling, it is assumed that the magnetic field inside the wiggler is given by:

$$B_x(s) = B_0 \sin(k_p s), \quad (3)$$

where B_0 is the peak field and is given by

$$B_0 = \frac{K}{93.4\lambda} = \begin{cases} 0.1438 & \text{at } 100 \text{ MeV,} \\ 0.4069 & \text{at } 150 \text{ MeV,} \\ 0.53 & \text{at } 200 \text{ MeV,} \end{cases} \quad (4)$$

Here $k_p = 2\pi/\lambda = 104.72$, $K = \sqrt{2}a_w$ and s is the longitudinal coordinate. Clearly, the different energies and undulator gaps mean that a whole range of K values and hence B_0 and magnetic fields $B_x(s)$ need to be considered. However, we will show that the worst case, the case where the bend angle of all the dipoles in the undulator of total length L is greatest, still gives roughly the same amount of focusing present in a drift. This gives the following integrals which have to be the same in the model:

$$\int_0^L B_x(s) ds = 0 \text{ Tm}, \quad (5)$$

$$\int_0^L B_x^2(s) ds = 0.0397269 \text{ T}^2 \text{m}, \quad (6)$$

and which were found to be identical. This was achieved by choosing the dipoles to be of length $l_{\text{dip}} = \lambda/4$ and hence the drift lengths between dipoles was $l_{\text{drift}} = (\lambda - 2l_{\text{dip}})/2$ which gives the bend angle for each dipole to be 0.0125 rad so each dipole in the model of the wiggler bends by approximately half a degree. For the purposes of the plots, the initial Twiss parameters were taken to be $\beta_x = \beta_y = 10\text{m}$ and $\alpha_x = \alpha_y = 0$. We compared the results of matching with the undulator modelled properly to matching the same section of beamline with a drift instead of the undulator. Simulations show that the match can be done with a drift as the strengths are comparable. However, for a correct model, the proper undulator model should be implemented.

Further, because there is some uncertainty as to the initial Twiss parameters, these were varied over a range up to 1000 m for β_x and β_y and $[-50 : 50]$ for α_x and α_y . All were varied both independently and together so as to cover all possible settings over the ranges described. This was done with sufficient resolution to ensure all matches could be achieved. The strengths of the quadrupoles were within the prescribed ranges set by the specifications. Whilst the match was shown to be achievable for all ranges considered, the middle of the chicane does behave very much like a drift. Therefore, the higher β_x and β_y are at the start of the considered section, the higher they will be at the exit of this section. Moreover, the higher the values of the Twiss parameters at the start are, the less precise the waist at the centre of the undulator is and the larger the beam is at the entrance and exit of the undulator due to the β functions having parabolatype shapes throughout the centre of the chicane. This is almost entirely independent of the choice of α functions at the entrance of the line.

CONCLUSION

Based on the analytical calculations given in [4, 11], we have estimated the microbunching gain for one of the CLARA modes of operation. Given the relatively low maximum energy of CLARA as compared with larger FEL facilities, and our single-chicane compression, it is not expected that the microbunching instability will have a great detrimental effect on the quality of the electron bunch at the entrance to the FEL. However, as CLARA is a test-bed for future FEL technology in the UK, valuable experience would be gained from operating a laser heater, and so it may be beneficial to install one. Investigations of alternative methods of damping microbunching to replace the laser heater are also in progress, such as reversible heating using bending magnets [13] or a transverse gradient undulator [14], as these may be more suitable for the low slice energy spread requirements of FEL seeding schemes. We have also proposed a method of inducing the microbunching instability, in order to control it, and to learn how it develops under different conditions.

REFERENCES

- [1] J. A. Clarke *et al.* “CLARA conceptual design report”. *Journal of Instrumentation*, 9(05):T05001, 2014.
- [2] D. Ratner *et al.* Time-resolved imaging of the microbunching instability and energy spread at the linac coherent light source. *Phys. Rev. ST Accel. Beams*, 18:030704, Mar 2015.
- [3] J. Lee *et al.* Pal-xfel laser heater commissioning. *Nucl. Instrum. Meth. A*, Nov 2016.
- [4] Z. Huang and K.-J. Kim. Formulas for coherent synchrotron radiation microbunching in a bunch compressor chicane. *Phys. Rev. ST Accel. Beams*, 5:074401, Jul 2002.
- [5] S. Bettoni *et al.* “Microbunching instability studies in Swiss-FEL”. *Proceedings of IPAC’12, New Orleans, USA*, 2012.
- [6] S. Seletskiy *et al.* Seeding, controlling, and benefiting from the microbunching instability. *Phys. Rev. Lett.*, 111:034803, Jul 2013.
- [7] Y. M. Saveliev *et al.* Characterisation of electron bunches from alice (erlp) dc photoinjector gun at two different laser pulse lengths. *Proceedings of EPAC’08, Genova, Italy*, 2008.
- [8] L. Yan *et al.* Ultrashort electron bunch train production by uv laser pulse stacking. *Proceedings of IPAC’10, Kyoto, Japan*, 2010.
- [9] Z. Huang *et al.* Measurements of the linac coherent light source laser heater and its impact on the x-ray free electron laser performance. *Phys. Rev. ST Accel. Beams*, 13:020703, Feb 2010.
- [10] S. Spampinati *et al.* Laser heater commissioning at an externally seeded free-electron laser. *Phys. Rev. ST Accel. Beams*, 17:120705, Dec 2014.
- [11] Z. Huang *et al.* Suppression of microbunching instability in the linac coherent light source. *Phys. Rev. ST Accel. Beams*, 7:074401, Jul 2004.
- [12] H. Grote and F. C. Iselin. “the mad program, v8.1. CERN/SL/90-13(AP) (Rev. 5), 1993.
- [13] G. Stupakov and P. Emma. “Reversible electron beam heater without transverse deflecting cavities”. *Proceedings of FEL’15, Daejeon, Korea*, 2015.
- [14] C. Feng *et al.* “Suppression of microbunching instability via a transverse gradient undulator”. *New J Phys*, 17(7):073028, 2017.